$\tilde{X}\ ^3\Sigma^-$ and $\tilde{A}\ ^3\Pi$ Electronic States of Ketenylidene (CCO): Analysis of the Renner Effect in the Upper State†

Shawn T. Brown, Yukio Yamaguchi, and Henry F. Schaefer, III*

Center for Computational Quantum Chemistry, University of Georgia, Athens, Georgia 30602

Received: October 22, 1999; In Final Form: January 11, 2000

Ab initio electronic structure theory has been employed in order to systematically investigate the $\tilde{X}\ ^3\Sigma^-$ and $\tilde{A}\ ^3\Pi$ electronic states of ketenylidene (CCO). The total energies and physical properties including equilibrium geometries, dipole moments, harmonic vibrational frequencies, and associated infrared (IR) intensities of CCO were predicted using the SCF, CISD, CCSD, equation of motion coupled cluster with single and double excitations (EOM-CCSD), and CCSD(T) levels of theory with a wide range of basis sets. The $\tilde{X}\ ^3\Sigma^-$ state of CCO is linear at equilibrium. The potential energy surface of the $\tilde{A}\ ^3\Pi$ state of CCO splits into $^3A''$ and $^3A'$ states on bending and each surface has its own minimum at the linear configuration, i.e., this state is a type A Renner−Teller state in the nomenclature of Lee, Fox, Schaefer, and Pitzer.[1] The two harmonic bending frequencies for the two surfaces of the $\tilde{A}\ ^3\Pi$ state were determined via the EOM-CCSD method. From the harmonic vibrational frequencies of the $\tilde{A}\ ^3\Pi$ state, the Renner parameter (ϵ), and the average harmonic bending frequency ω_2 can easily be determined. At the EOM-CCSD TZ3P(2f) level of theory, values of -0.153 and 627 cm^{-1} were determined for ϵ and ω_2, respectively, which are in good agreement with experimentally determined values in both sign and magnitude. Theoretically predicted harmonic stretching vibrational frequencies were in close agreement with experimental fundamental frequencies, indicating relatively small anharmonicities. At the CCSD(T) level of theory with the largest basis set, Dunning's cc-pVQZ, the classical $\tilde{X}-\tilde{A}$ splitting (T_e value) was predicted to be 33.1 kcal/mol, and the quantum mechanical splitting (T_0 value) to be 34.0 kcal/mol which are in excellent agreement with the experimental T_0 values of 33.3 kcal/mol by Devillers and Ramsay (in 1971), 33.3 kcal/mol by Fujitake, Kiryu, and Ohashi (in 1992), 33.9 kcal/mol by Zengin, Persson, Strong, and Continetti (in 1996), and 33.3 kcal/mol by Fulara, Grutter, Wyss, and Maier (in 1998).

I. Introduction

The CCO molecule is a reactive intermediate involved in many chemical reactions in the gas phase.[2] This molecule has also been identified in interstellar dark clouds by microwave spectroscopy.[3] The first spectroscopic study of the free radical CCO using the matrix-isolated infrared (IR) technique was performed by Jacox, Milligan, Moll, and Thompson in 1965.[4] CCO has been prepared via the photolysis of matrix-isolated cyanogen azide (N_3CN) in the presence of CO at wavelengths shorter than 2000 Å. This species was also produced by vacuum ultraviolet photolysis of matrix-isolated carbon suboxide (C_3O_2). Jacox et al. observed the three vibrational fundamentals of CCO in an argon matrix at 381, 1074, and 1978 cm^{-1}. Isotopic studies were consistent with a linear structure for CCO.[4]

The absorption spectrum in the region 5000 to 6500 Å was observed by Devillers[5] during the flash photolysis of carbon suboxide and was tentatively attributed to the CCO molecule. These observations were extended to 9000 Å, and rotational and vibrational analyses of some of the bands were carried out by Devillers and Ramsay.[6] The strong band near 8580 Å (11650 cm^{-1}) was assigned as the 000−000 band. This assignment was confirmed by an independent investigation using isotopically labeled species. They also reported the three fundamental vibrational frequencies $\nu_1 = 2045.7$, $\nu_2 = 607.8$, and $\nu_3 = 1270$ cm^{-1} for the $\tilde{A}\ ^3\Pi$ state and one fundamental frequency $\nu_2 = 379.4$ cm^{-1} for the $\tilde{X}\ ^3\Sigma^-$ state. The mode ν_2 corresponded to the bending motion of the molecule. The rotational analyses of the bands proved that both electronic states exhibit linear geometries and the magnitudes of the rotational constants were consistent only with a triatomic species. The absence of any intensity alternation or missing lines in the spectrum proved that the molecule does not have a center of symmetry. From all the available evidence Devillers and Ramsay concluded that the spectrum indeed arises from the $\tilde{A}\ ^3\Pi_i-\tilde{X}\ ^3\Sigma^-$ transition of the CCO molecule.

DeKock and Weltner reported a matrix-isolated IR study of CCO, CNN, and C_3O molecules.[7] The vaporized carbon atoms were condensed with an argon:CO mixture (200:1) onto a CsI window at 4 K. Bands for CCO were observed at 1969 ($^{12}C^{12}C^{16}O$), 1934 ($^{12}C^{12}C^{18}O$), and 1928 plus 1021 cm^{-1} ($^{13}C^{12}C^{18}O$). From the derived stretching force constants of the two isoelectronic molecules, CCO and CNN, they pointed out that these molecules have the different chemical bonding C−C═O vs C≡N═N. Smith and Weltner also reported electron spin resonance (ESR) spectra of the triplet molecules CCO and CNN in rare-gas matrixes.[8] Pitts, Donnelly, Baronavski, and McDonald reported[2] laser induced excitation and fluorescence spectra of CCO ($\tilde{A}\ ^3\Pi \leftrightarrow \tilde{X}\ ^3\Sigma^-$). Values of 1967 and 1063 cm^{-1} were found for the ν_1 and ν_3 stretching vibrations in the $\tilde{X}\ ^3\Sigma^-$ state.

In order to obtain further information on rovibronic energy level structures and vibronic interactions in the $\tilde{A}$ electronic

† Part of the special issue "Marilyn Jacox Festschrift".

10.1021/jp9937712 CCC: $19.00
Published on Web 02/26/2000

excited state, the $\tilde{A}(000)-\tilde{X}(000)$, $\tilde{A}(010)-\tilde{X}(000)$, and $\tilde{A}(010)-\tilde{X}(010)$ band spectra of CCO were reinvestigated by means of near-infrared diode laser spectroscopy by Fujitake et al.,[9] Ohashi et al.,[10] and Abe et al.[11] to determine detailed molecular constants for the $\tilde{A}(000)$, $\tilde{X}(010)$, and $\tilde{A}(010)$ states. They measured the origin of the $\tilde{A}\ ^3\Pi \leftrightarrow \tilde{X}\ ^3\Sigma^-$ band to be 11651.182 cm^{-1}, which is consistent with the value by Devillers and Ramsay.[6] Recently the same Kanazawa group reported the $\tilde{A}(020)\kappa^3\Pi-\tilde{X}\ ^3\Sigma^-(000)$ and $\tilde{A}\ ^3\Pi_i(001)-\tilde{X}\ ^3\Sigma^-(000)$ bands of the CCO radical by using two laser systems in the region from 12881 to 13043 cm^{-1}.[12]

Zengin, Persson, Strong, and Continetti investigated the low-lying states of CCO by photoelectron spectroscopy of CCO^- at wavelengths of 266 and 355 nm.[13] Photodetachment was observed to occur to the $\tilde{X}\ ^3\Sigma^-$, $\tilde{A}\ ^3\Pi$, $\tilde{a}\ ^1\Delta$, and $\tilde{b}\ ^1\Sigma^+$ electronic states of CCO. Their work marked the first observation of the low-lying singlet states. The $\tilde{X}-\tilde{A}$ energy separation was found to be 1.468 eV in the 266 nm spectrum. The 0.024 eV difference from the previous spectroscopic determinations may have arisen from nonlinearities in the eKE calibration. A revised value for the electron affinity of CCO is found to be 2.289 ± 0.018 eV. Using the measured electron affinity of CCO, the heats of formation $\Delta H^0_{f,298}$ (CCO) $= 3.99 \pm 0.20$ eV and $\Delta H^0_{f,298}$ (CCO^-) $= 1.67 \pm 0.20$ eV were determined. In addition, the C−CO bond dissociation energy in CCO was determined to be D_{298} (C−CO) $= 2.29 \pm 0.20$ eV. Zengin's experimental results were compared with new CASPT2 calculations on the electronic structure of both CCO and CCO^-.

In 1998, Fulara, Grutter, Wyss, and Maier studied $\tilde{A}\ ^2\Sigma^+ \leftarrow \tilde{X}\ ^2\Pi$ electronic absorption spectrum of CCO^- in a neon matrix.[14] The $\tilde{A}\ ^3\Pi \leftarrow \tilde{X}\ ^3\Sigma^-$ electronic absorption spectrum of the CCO radical was formed after irradiation of the neon matrix containing CCO^- with UV light ($\lambda \geq 300$ nm). The vibrational frequencies $\nu_1 = 2045$ and $\nu_3 = 1279$ cm^{-1} in the $\tilde{A}\ ^3\Pi$ excited state measured from this spectrum and the 0_0^0 band at 11650 cm^{-1} are very similar to the values from the gas phase spectrum.[6]

Choi, Mordaunt, Bise, Taylor, and Neumark investigated the triplet and singlet states of the CCO radical using fast radical beam photofragment translational spectroscopy, in which CCO is generated by laser photodetachment of CCO^- and subsequent photodissociation, and anion photoelectron spectroscopy.[15] They determined the bond dissociation energy for C−CO to be D_0 (C−CO) $= 2.24 \pm 0.02$ eV (51.7 ± 0.5 kcal/mol) and the heat of formation to be $\Delta H^0_{f,298}$ (CCO) $= 4.04 \pm 0.02$ eV (91.1 ± 0.5 kcal/mol). For other experimental studies on CCO readers should refer to the superb compilation by Jacox.[16]

There are several theoretical studies on the CCO radical.[17−21] In 1985, Chabalowski, Buenker, and Peyerimhoff examined the $\tilde{X}\ ^3\Sigma^-$, $\tilde{A}\ ^3\Pi$, $1\ ^1\Sigma^+$, $1\ ^1\Delta$, $1\ ^1\Pi$, $2\ ^1\Pi$ states of the CCO radical with an MRD-CI treatment with configuration selection and energy extrapolation to determine vertical excitation energies and transition probabilities.[18] The extrapolated geometric parameters for the $\tilde{X}\ ^3\Sigma^-$ state from their study were 1.3676 Å for r_e (CC) and 1.1648 Å for r_e (CO). DeKock, Grev, and Schaefer studied the isovalent molecules CCO, CNN, SiCO, and SiNN in their triplet linear ground states employing SCF, CISD, and CASSCF wave functions with the DZ+P and TZ+2P basis sets.[19] They discussed the bonding of the C or Si atom with the CO or N_2 ligand and concluded that the strongest bond is formed between the C and N atoms in CNN and the weakest between the Si and N atoms in SiNN. Their theoretical results were easily brought into harmony for CCO and SiCO, but not for CNN and SiNN. Maclagan and Sudkeaw looked at the relative energetics between CCO and its cation with MP4SDQ/6-311G** at geometries determined at the MP2/6-31G** level of theory.[20] Suter, Huang, and Engels reported a MRD-CI study of the hyperfine structure of the ground-state CCO, CNN, and NCN molecules.[21] The geometries and harmonic vibrational frequencies were obtained with the QCISD method.

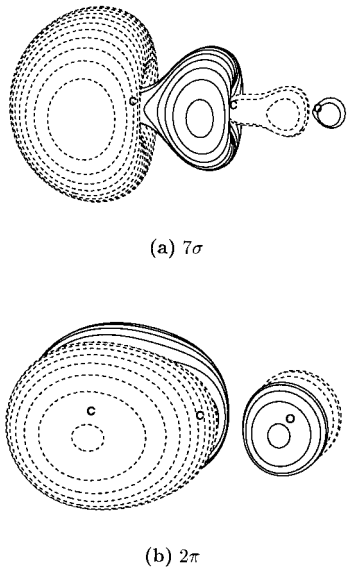

Figure 1. The 7σ and 2π molecular orbitals for the $\tilde{X}\ ^3\Sigma^-$ ground state of CCO determined at the TZ3P(2f) SCF level of theory.

The importance of the CCO radical as a reactive intermediate and an interstellar molecule warrants its further theoretical consideration. It is to this purpose that high-level configuration interaction and coupled-cluster methods are used in the present study to examine the properties and energetics of the $\tilde{X}\ ^3\Sigma^-$ and $\tilde{A}\ ^3\Pi$ states of CCO.

II. Electronic Structure Considerations

The ground state of the linear CCO radical has the electronic configuration:

$$[\text{core(CCO)}](4\sigma)^2(5\sigma)^2(6\sigma)^2(1\pi)^4(7\sigma)^2(2\pi_i)(2\pi_o) \quad \tilde{X}\ ^3\Sigma^- \quad (1)$$

where [core(CCO)] denotes the three core (C and O: 1s-like) orbitals, and π_i and π_o stand for the in-plane and out-of-plane π molecular orbitals (MOs). The 4σ and 5σ MOs describe the C−O and C−C σ bonds, while the 6σ and 7σ MOs are the lone pair orbitals on the O atom and C atom, respectively. The 1π and 2π MOs are associated with the C−O and C−C π bonds. The 7σ and 2π MOs are depicted in Figure 1a and b. The ground state has a degenerate real bending frequency.

The first excited triplet state of CCO has the electronic configuration

$$[\text{core(CCO)}](4\sigma)^2(5\sigma)^2(6\sigma)^2(1\pi)^4(7\sigma)(2\pi_i)^2(2\pi_o) \quad \tilde{A}\ ^3\Pi \quad (2)$$

or

$$[\text{core(CCO)}](4\sigma)^2(5\sigma)^2(6\sigma)^2(1\pi)^4(7\sigma)(2\pi_o)^2(2\pi_i) \quad \tilde{A}\ ^3\Pi \quad (3)$$

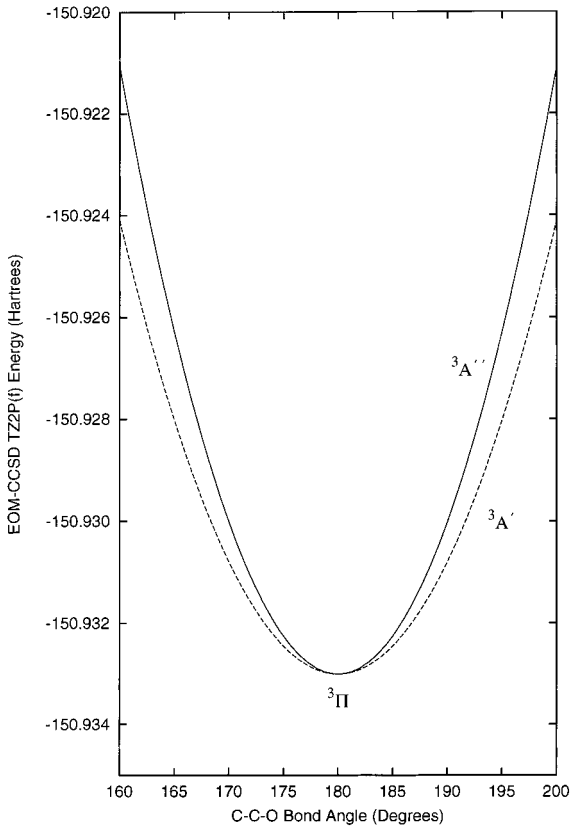

Figure 2. The harmonic bending potentials for the $\tilde{A}\ ^3\Pi$ state of CCO determined at the EOM-CCSD TZ2P(f) level of theory. From the Renner−Teller splitting, $^3A'$ and $^3A''$ states arise and this splitting is demonstrated by determining the energy of the two states at varying CCO bond angles with fixed bond lengths. The fact that the $^3A''$ potential lies higher in energy than the $^3A'$ surface indicates a negative ϵ value.

which is a single electron excitation relative to the ground state

$$(7\sigma)^2(2\pi)^2 \rightarrow (7\sigma)(2\pi)^3 \tag{4}$$

This state is predicted to possess the two distinct vibrational frequencies (674 and 578 cm^{-1} with the TZ3P(2f) EOM-CCSD method) along the CCO bending coordinate. Thus, the $\tilde{A}\ ^3\Pi$ state of CCO may be classified as a type A Renner−Teller molecule as proposed by Lee, Fox, Schaefer, and Pitzer.[1] The total energies of the $^3A''$ and $^3A'$ components for the $\tilde{A}\ ^3\Pi$ state with respect to the bond angle at the TZ2P(f) EOM-CCSD level of theory are illustrated in Figure 2.

At this point, it may be useful to analyze the molecular orbital (MO) Hessian (the second derivatives of the SCF electronic energy with respect to MO rotations)[22] of the reference self-consistent-field (SCF) wave functions. At the linear configuration the MO Hessian of the $\tilde{X}\ ^3\Sigma^-$ state of CCO shows all positive eigenvalue as expected. Thus, the SCF wave function for the $\tilde{X}\ ^3\Sigma^-$ state of CCO is *stable*. The $\tilde{A}\ ^3\Pi$ state of CCO has one zero and one negative eigenvalue of the MO Hessian. The eigenvector of the zero eigenvalue is related to the $2\pi_i-2\pi_o$ MO rotation, indicating that the SCF energy is not altered by exchanging the $2\pi_i$ and $2\pi_o$ orbitals. The eigenvector of the negative eigenvalue corresponds to the $7\sigma-2\pi$ MO rotation. The SCF wave function of the $\tilde{A}\ ^3\Pi$ state of CCO is, therefore, *unstable* and there is one lower-lying state ($\tilde{X}\ ^3\Sigma^-$, which is obtained by exchanging the 7σ and 2π orbitals) at this equilibrium geometry. Consequently, the physical properties which involve the $7\sigma-2\pi$ MO rotation should be interpreted with great caution for the $\tilde{A}\ ^3\Pi$ state.[22−24]

For the ground state ($\tilde{X}\ ^3\Sigma^-$), the degenerate bending motions lower the molecular symmetry to C_s symmetry and the electronic state to $^3A''$. On the other hand, for the first excited triplet state, the one bending motion (denoted ω_2^- due to the bending motion being antisymmetic with respect to the plane of the singly occupied orbital) leads the $\tilde{A}\ ^3\Pi$ state to a $^3A''$ state and the other bending motion (denoted ω_2^+ due to the bending motion being symmetric with respect to the plane of the singly occupied orbital) to a $^3A'$ state. In C_s symmetry, therefore, the ground state and one component ($^3A''$) of the first excited triplet state interact with each other. Therefore, the ω_2^- bending vibrational frequency of the first excited triplet state should not be determined as the first root of correlated wave functions (vide infra). However, the ω_2^+ bending vibrational frequency of the first excited triplet state may be obtained without concern regarding variational collapse.

III. Renner−Teller Effects

As mentioned earlier, the CCO bending vibrational mode of the $\tilde{A}\ ^3\Pi$ state is subject to the Renner−Teller effect.[25−29] The Renner−Teller effect arises from the splitting of the bending potential into "plus" (V^+) and "minus" (V^-) potentials. The V^+ potential corresponds to the electronic state that is symmetric under reflection in the plane of the bent molecule and V^- to the antisymmetric state.[25,30] In this case, the splitting is the result of whether the configuration is $(2\pi_i)^2(2\pi_o)^1$ or $(2\pi_i)^1(2\pi_o)^2$. Referring to ref 27, the zeroth-order bending potential function, neglecting anharmonic terms, is written as the mean of the V^+ and V^- potentials

$$V^0 = ar^2 = \frac{V^+ + V^-}{2} \tag{5}$$

A splitting function may also be defined, and it has the similar form as the V^0

$$V^+ - V^- = \alpha r^2 \tag{6}$$

It is important to note that a is the force constant for the zeroth-order bending potential and α is the force constant for the splitting function and its sign is dependent on whether the V^+ surface lies above or below the V^- surface. The Renner parameter ϵ is a dimensionless constant used to describe the Renner−Teller splitting of the potential and is defined as

$$\epsilon = \frac{\alpha}{2a} = \frac{V^+ - V^-}{V^+ + V^-} \tag{7}$$

The sign of epsilon is therefore dependent on the sign of α, i.e., the relative ordering of the V^+ and V^- surfaces. By defining the force constant of V^+ to be f^+ and f^- to be that for V^- it can be shown that

$$V^+ = V^0 + \frac{V^+ - V^-}{2} = \left(a + \frac{\alpha}{2}\right)r^2 = f^+r^2 \tag{8}$$

$$V^- = V^0 - \frac{V^+ - V^-}{2} = \left(a - \frac{\alpha}{2}\right)r^2 = f^-r^2 \tag{9}$$

Combining eqs 7−9, the Renner parameter may be expressed as

$$\epsilon = \frac{f^+ - f^-}{f^+ + f^-} \tag{10}$$

TABLE 1: Theoretical Predictions of the Total Energy (in hartree), Dipole Moment (in debye), Harmonic Vibrational Frequencies (in cm^{-1}), Infrared (IR) Intensities (in parentheses in km mol^{-1}), and Zero-Point Vibrational Energy (ZPVE in kcal/mol) for the $\tilde{X}\ ^3\Sigma^-$ State of the CCO Molecule[a]

level of theory	energy	μ_e	ω_1 (σ)	ω_2 (π)	ω_3 (σ)	ZPVE
TZ2P SCF	−150.509 249	1.384	2282(712.0)	538(119.0)	1123(1.4)	6.41
TZ2P+diff SCF	−150.510 065	1.380	2283(719.6)	540(117.6)	1125(1.3)	6.42
TZ3P SCF	−150.511 238	1.364	2289(706.6)	540(115.3)	1134(1.1)	6.44
TZ2P(f) SCF	−150.515 265	1.378	2297(713.3)	544(123.5)	1136(1.1)	6.46
TZ2P(f)+diff SCF	−150.515 986	1.375	2298(720.0)	543(119.4)	1137(0.9)	6.46
TZ3P(2f) SCF	−150.516 418	1.370	2294(705.8)	542(116.3)	1132(1.0)	6.45
TZ2P CISD	−150.905 539	1.452	2148(377.0)	457(87.5)	1087(2.0)	5.93
TZ2P+diff CISD	−150.906 918	1.449	2148(380.5)	457(85.7)	1089(2.2)	5.93
TZ3P CISD	−150.912 169	1.429	2159(374.0)	457(83.7)	1106(2.4)	5.97
TZ2P(f) CISD	−150.943 391	1.429	2184(375.0)	472(93.1)	1120(2.9)	6.07
TZ2P(f)+diff CISD	−150.944 592	1.426	2185(377.5)	472(89.4)	1122(3.2)	6.08
TZ3P(2f) CISD	−150.954 033	1.419	2173(376.6)	466(88.1)	1115(2.8)	6.03
TZ2P CCSD	−150.949 505		2044	413	1064	5.62
TZ2P+diff CCSD	−150.951 010		2045	411	1066	5.62
TZ3P CCSD	−150.956 783		2057	411	1084	5.67
TZ2P(f) CCSD	−150.991 011		2083	427	1099	5.77
TZ2P(f)+diff CCSD	−150.992 324		2084	427	1101	5.77
TZ3P(2f) CCSD	−151.002 750		2069	420	1092	5.72
TZ2P CCSD(T)	−150.971 415		1980	392	1038	5.43
TZ2P+diff CCSD(T)	−150.972 990		1980	399	1039	5.46
TZ3P CCSD(T)	−150.979 293		1994	371	1058	5.42
TZ2P(f) CCSD(T)	−151.014 854		2020	409	1073	5.59
TZ2P(f)+diff CCSD(T)	−151.016 225		2021	442	1074	5.69
TZ3P(2f) CCSD(T)	−151.027 818		2003	455	1066	5.69
exptl ref 4 (1965)			1978	381	1074	
exptl ref 6 (1971)				379.4		
exptl ref 7 (1971)			1969			
exptl ref 2 (1981)			1967		1063	
exptl ref 54 (1986)			1970.86			
exptl ref 10 (1993)				379.53		
exptl ref 11 (1994)				379.53		
exptl ref 55 (1997)			1970.86			
exptl ref 14 (1998)			1972.5			

[a] IR intensities of ω_2 mode were doubled.

On the other hand the ω^+ and ω^- bending frequencies are related to ϵ by

$$\epsilon = \frac{(\omega^+)^2 - (\omega^-)^2}{(\omega^+)^2 + (\omega^-)^2} \tag{11}$$

Experimentally, ϵ is determined from the assignment of vibronic energy levels from the splittings observed in the spectra. In triplet states, spin−orbit effects also contribute to the splitting. The actual bending mode observed experimentally is a combination of the ω_2^+ and ω_2^- modes and is determined from the zeroth-order bending potential

$$\omega_2 = \frac{1}{2\pi c}\sqrt{\frac{a}{\mu}} \tag{12}$$

where a is the force constant defined by eq 5 and μ is the kinetic energy contribution of the bending motion.

The bending potential is determined as an average of the two split potentials. Devillers and Ramsay determined a value for ϵ of −0.172 and for ω_2 of 607.8 cm^{-1} from their spectrum obtained via the flash photolysis of carbon suboxide.[6] Later Abe et al. determined values of 0.176 and 594.7514(19) cm^{-1} for ϵ and ω_2, respectively.[11] The difference in the sign of ϵ is due to the fact that Abe et al. did not consider the sign in their analysis. With the definition of the potentials given above, the $^3A'$ state should be assigned to the V^+ surface and the $^3A''$ to the V^- surface. This then agrees with Devillers and Ramsay's conclusion that ϵ has a negative value, for it is clear from Figure 2 that V^- lies above the V^+ surface. It is important to note that Beaton and Brown have found that NCN, which is isoelectronic to CCO, also has a negative ϵ value.[31] The magnitudes of the ϵ values determined with the EOM-CCSD method show good agreement with both experimental values.

IV. Theoretical Procedures

Six basis sets were employed in order to optimize geometries and to determine physical properties. The basis sets of valence triple-ζ (TZ) quality for C and O are obtained from Dunning's triple-ζ contraction[32] of Huzinaga's primitive Gaussian set[33] and are designated (10s6p/5s3p). The orbital exponents of the polarization functions are α_d(C) = 1.50 and 0.375 and α_d(O) = 1.70 and 0.425 for double polarization (TZ2P), and α_d(C) = 3.00, 0.75, 0.1875 and α_d(O) = 3.40, 0.85, 0.2125 for triple polarization (TZ3P). The orbital exponents of the higher angular momentum functions are α_f(C) = 0.80 and α_f(O) = 1.40 for one set of higher angular momentum functions [TZ2P(f)], and α_f(C) = 1.60, 0.40, and α_f(O) = 2.80, 0.70 for two sets of higher angular momentum functions [TZ3P(2f)]. The orbital exponents of the diffuse functions are α_p(C) = 0.03389 and α_s(C) = 0.04812 and α_p(O) = 0.05840 and α_s(O) = 0.08993 for one set of diffuse functions [TZ2P+diff and TZ2P(f)+diff]. Pure angular momentum d and f functions were used throughout. The largest basis set, TZ3P(2f), comprises 129 contracted Gaussian functions for CCO with a contraction scheme of C and O (10s6p3d2f/5s3p3d2f). Three corelation consistent polarized valence basis sets developed by Dunning,[34] cc-pVDZ, cc-pVTZ, and cc-pVQZ, have been also employed for single point

$\tilde{X}\ ^3\Sigma^-$ State

1.3639	1.1222	TZ2P SCF
1.3638	1.1221	TZ2P+diff SCF
1.3628	1.1237	TZ3P SCF
1.3614	1.1223	TZ2P(f) SCF
1.3612	1.1223	TZ2P(f)+diff SCF
1.3618	1.1221	TZ3P(2f) SCF
1.3682	1.1430	TZ2P CISD
1.3680	1.1429	TZ2P+diff CISD
1.3668	1.1449	TZ3P CISD
1.3615	1.1425	TZ2P(f) CISD
1.3610	1.1424	TZ2P(f)+diff CISD
1.3616	1.1417	TZ3P(2f) CISD
1.3716	1.1547	TZ2P CCSD
1.3713	1.1547	TZ2P+diff CCSD
1.3700	1.1568	TZ3P CCSD
1.3643	1.1543	TZ2P(f) CCSD
1.3638	1.1543	TZ2P(f)+diff CCSD
1.3649	1.1536	TZ3P(2f) CCSD
1.3769	1.1635	TZ2P CCSD(T)
1.3765	1.1635	TZ2P+diff CCSD(T)
1.3751	1.1657	TZ3P CCSD(T)
1.3692	1.1630	TZ2P(f) CCSD(T)
1.3686	1.1631	TZ2P(f)+diff CCSD(T)
1.3699	1.1627	TZ3P(2f) CCSD(T)

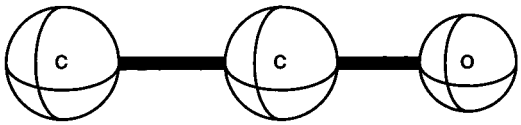

Figure 3. Optimized geometries for $\tilde{X}\ ^3\Sigma^-$ CCO determined by 24 theoretical methods employed in this research. Bond distances are in angstroms.

energy calculations. The cc-pVQZ basis set consists of 165 contracted Gaussian functions with a contraction scheme of C and O (12s6p3d2f1g/5s4p3d2f1g).

The zeroth-order descriptions of the $\tilde{X}\ ^3\Sigma^-$ and $\tilde{A}\ ^3\Pi$ states of CCO were obtained using one-configuration SCF (restricted Hartree−Fock) wave functions. Correlation effects were included using configuration interaction with single and double excitations (CISD), coupled cluster with single and double excitations (CCSD),[35,36] and CCSD with perturbative triple excitations [CCSD(T)][37,38] levels of theory. In all correlated procedures with the valence TZ quality basis sets, the three core (C and O: 1s-like) orbitals were frozen and the three highest-lying virtual (C and O: 1s*-like) orbitals were deleted. With the TZ3P(2f) basis set, the numbers of configuration state functions (CSFs) in the CISD procedures in the Hartree−Fock interacting space[39,40] are 107 388 for the $\tilde{X}\ ^3\Sigma^-$ state of CCO in C_{2v} symmetry and 211 230 in C_s symmetry, 107 300 for the $\tilde{A}\ ^3\Pi$ state of CCO in C_{2v} symmetry and 210 988 in C_s symmetry. At the TZ3P(2f) CISD optimized geometries, single-point CISD energies were computed with the three correlation consistent basis sets (cc-pVDZ, cc-pVTZ, and cc-pVQZ) by freezing the three core orbitals only. With the cc-pVQZ basis set the numbers of CSFs in the CISD procedures are 190 782 for the $\tilde{X}\ ^3\Sigma^-$ state and 190 586 for the $\tilde{A}\ ^3\Pi$ state in C_{2v} symmetry, respectively.

The EOM-CCSD wave function[41] was utilized for the study of the $\tilde{A}\ ^3\Pi$ state. The EOM−CCSD wave function does not suffer from the orbital instability problem mentioned in the prior section due to the fact that the excited-state energies are determined as higher roots of the ground state CCSD wave function in the same symmetry. Therefore, it was possible to determine all harmonic vibrational frequencies for the first excited triplet state using this EOM-CCSD wave function. This fact allows the evaluation and analysis of the Renner−Teller

$\tilde{A}\ ^3\Pi$ State

1.2617	1.1436	TZ2P SCF
1.2619	1.1436	TZ2P+diff SCF
1.2616	1.1450	TZ3P SCF
1.2611	1.1432	TZ2P(f) SCF
1.2611	1.1432	TZ2P(f)+diff SCF
1.2607	1.1432	TZ3P(2f) SCF
1.2679	1.1649	TZ2P CISD
1.2679	1.1650	TZ2P+diff CISD
1.2685	1.1666	TZ3P CISD
1.2651	1.1631	TZ2P(f) CISD
1.2650	1.1631	TZ2P(f)+diff CISD
1.2642	1.1626	TZ3P(2f) CISD
1.2792	1.1712	TZ2P EOM-CCSD
1.2794	1.1713	TZ2P+diff EOM-CCSD
1.2795	1.1730	TZ3P EOM-CCSD
1.2761	1.1696	TZ2P(f) EOM-CCSD
1.2761	1.1697	TZ2P(f)+diff EOM-CCSD
1.2755	1.1692	TZ3P(2f) EOM-CCSD
1.2725	1.1791	TZ2P CCSD
1.2726	1.1792	TZ2P+diff CCSD
1.2733	1.1807	TZ3P CCSD
1.2696	1.1770	TZ2P(f) CCSD
1.2696	1.1771	TZ2P(f)+diff CCSD
1.2689	1.1768	TZ3P(2f) CCSD
1.2776	1.1877	TZ2P CCSD(T)
1.2777	1.1878	TZ2P+diff CCSD(T)
1.2784	1.1894	TZ3P CCSD(T)
1.2745	1.1854	TZ2P(f) CCSD(T)
1.2744	1.1856	TZ2P(f)+diff CCSD(T)
1.2739	1.1856	TZ3P(2f) CCSD(T)

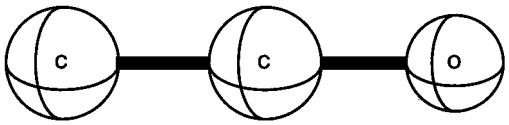

Figure 4. Optimized geometries for $\tilde{A}\ ^3\Pi$ CCO determined by 30 theoretical methods employed in this research. Bond distances are in angstroms.

splitting in the CCO bending mode. It was also important to examine the performance of EOM-CCSD in determining the structure, harmonic vibrational frequencies, and energetics of $\tilde{A}\ ^3\Pi$ CCO in comparison to the CCSD and CCSD(T) levels of theory.

The structures of the three stationary points were optimized using analytic derivative methods.[42−44] Harmonic vibrational frequencies at the SCF level were calculated analytically, while at the CISD level of theory they were obtained by finite differences of analytic gradients. For the CCSD, EOM-CCSD and CCSD(T) methods the equilibrium geometries and harmonic vibrational frequencies were determined by five point numerical differentiation of total energies. At the TZ3P(2f) CCSD, EOM-CCSD, and CCSD(T) optimized geometries, single-point CCSD, EOM-CCSD, and CCSD(T) energies were computed with the three correlation consistent basis sets by freezing the three core orbitals only. Computations were carried out using the PSI 2.0.8 program package[45] on IBM RS/6000 workstations. The computations based on the EOM-CCSD method were performed using the ACES II package.[46]

V. Results and Discussion

In Figure 3 the optimized geometries for $\tilde{X}\ ^3\Sigma^-$ CCO are shown at 24 levels of theory, and in Figure 4 the optimized geometries for $\tilde{A}\ ^3\Pi$ CCO are depicted at 30 levels of theory. The total energies, dipole moments, harmonic vibrational frequencies, and associated infrared (IR) intensities of the $\tilde{X}\ ^3\Sigma^-$ and the $\tilde{A}\ ^3\Pi$ states of CCO are presented in Tables 1 and 2, respectively. Total energies at the CISD, CCSD, CCSD(T)

TABLE 2: Theoretical Predictions of the Total Energy (in hartree), Dipole Moment (in debye), Harmonic Vibrational Frequencies (in cm^{-1}), and Infrared Intensities (in parentheses in km mol^{-1}) for the $\tilde{A}\ ^3\Pi$ State of the CCO Molecule

level of theory	energy	μ_e	ω_1 (σ)	ω_2^-(π^-,A″)	ω_2^+(π^+,A′)	ω_3(σ)
TZ2P SCF	−150.457 935	1.583	2350(892.1)	819(28.9)	661(15.4)	1431(5.5)
TZ2P+diff SCF	−150.458 292	1.621	2348(902.3)	816(32.2)	660(15.1)	1430(5.6)
TZ3P SCF	−150.459 863	1.613	2361(882.6)	824(27.6)	662(13.6)	1437(5.8)
TZ2P(f) SCF	−150.464 831	1.579	2368(894.3)	833(30.8)	667(16.3)	1437(5.4)
TZ2P(f)+diff SCF	−150.465 176	1.613	2367(907.2)	826(35.9)	666(15.3)	1437(5.5)
TZ3P(2f) SCF	−150.465 824	1.596	2365(889.4)	832(31.0)	664(13.7)	1435(5.6)
TZ2P CISD	−150.851 254	1.440	2211(510.9)		594(7.5)	1359(8.2)
TZ2P+diff CISD	−150.852 167	1.481	2210(518.4)		593(7.2)	1358(8.3)
TZ3P CISD	−150.857 790	1.462	2227(507.9)		592(6.5)	1367(8.5)
TZ2P(f) CISD	−150.890 591	1.452	2257(517.6)		610(8.3)	1376(8.4)
TZ2P(f)+diff CISD	−150.891 418	1.490	2256(526.2)		610(7.5)	1376(8.6)
TZ3P(2f) CISD	−150.901 182	1.474	2245(520.4)		603(6.8)	1372(8.7)
TZ2P EOM-CCSD	−150.889 760		2146	666	570	1307
TZ2P+diff EOM-CCSD	−150.890 772		2127	647	553	1303
TZ3P EOM-CCSD	−150.896 991		2164	664	567	1317
TZ2P(f) EOM-CCSD	−150.933 009		2194	683	586	1326
TZ2P(f)+diff EOM-CCSD	−150.933 918		2193	678	586	1326
TZ3P(2f) EOM-CCSD	−150.944 672		2180	674	578	1321
TZ2P CCSD	−150.895 361		2085		558	1307
TZ2P+diff CCSD	−150.896 380		2084		556	1307
TZ3P CCSD	−150.902 543		2104		555	1317
TZ2P(f) CCSD	−150.938 270		2135		575	1327
TZ2P(f)+diff CCSD	−150.939 189		2134		575	1326
TZ3P(2f) CCSD	−150.949 920		2120		567	1321
TZ2P CCSD(T)	−150.917 606		2039		591	1270
TZ2P+diff CCSD(T)	−150.918 699		2037		549	1269
TZ3P CCSD(T)	−150.925 425		2058		549	1279
TZ2P(f) CCSD(T)	−150.962 325		2089		555	1289
TZ2P(f)+diff CCSD(T)	−150.963 308		2088		564	1289
TZ3P(2f) CCSD(T)	−150.975 221		2072		558	1283
exptl ref 6 (1971)			2045.7			1270
exptl ref 12 (1996)						1284
exptl ref 14 (1998)			2045			1279

TABLE 3: Total CISD, CCSD, EOM-CCSD (for $\tilde{A}\ ^3\Pi$ CCO only), and CCSD(T) Energies (in hartrees) for the $\tilde{X}\ ^3\Sigma^-$ and $\tilde{A}\ ^3\Pi$ States of CCO at the Optimized Geometries with the Corresponding Methods Using the TZ3P(2f) Basis Set

	electronic state	
level of theory	$\tilde{X}\ ^3\Sigma^-$	$\tilde{A}\ ^3\Pi$
cc-pVDZ CISD	−150.829 489	−150.773 730
cc-pVTZ CISD	−150.944 718	−150.890 943
cc-pVQZ CISD	−150.981 296	−150.928 339
cc-pVDZ CCSD	−150.868 824	−150.813 450
cc-pVTZ CCSD	−150.992 905	−150.939 121
cc-pVQZ CCSD	−151.032 056	−150.979 068
cc-pVDZ CCSD(T)	−150.885 327	−150.830 242
cc-pVTZ CCSD(T)	−151.017 417	−150.963 884
cc-pVQZ CCSD(T)	−151.058 652	−151.005 903
cc-pVDZ EOM-CCSD[a]		−150.807 903
cc-pVTZ EOM-CCSD[a]		−150.933 925
cc-pVQZ EOM-CCSD[a]		−150.974 023

[a] No ground state energies are given for the EOM-CCSD method because the ground state was used as a reference and therefore the EOM-CCSD energy is only caclulated for the excited state.

levels of theory for $\tilde{X}\ ^3\Sigma^-$ and $\tilde{A}\ ^3\Pi$ CCO and also EOM-CCSD level of theory for $\tilde{A}\ ^3\Pi$ CCO with the three Dunning's correlation consistent basis sets at geometries determined with the TZ3P(2f) basis are given in Table 3. In Table 4, the Renner parameter and ω_2 frequencies for the $\tilde{A}\ ^3\Pi$ state of CCO are presented at the EOM-CCSD level of theory. Excitation energies (T_0 and T_e values) determined at 42 levels of theory are shown in Table 5 and bond dissociation (C−CO) energies (D_e and D_0 values) for $\tilde{X}\ ^3\Sigma^-$ CCO are displayed in Table 6.

A. Geometries. The optimized geometries of the ground and first excited triplet states of CCO are depicted in Figure 3 and Figure 4, respectively. As seen in Figure 3, the CC and CO bond lengths of the ground state are elongated with improved treatments of correlation effects, as is usually the case.[47−50] With the TZ3P(2f) basis set the difference in the SCF and CCSD(T) bond lengths are 0.0081 (1.3699−1.3618) Å for the CC bond and 0.0406 (1.1627−1.1221) Å for the CO bond. It is observed that the CO bond is more sensitive to correlation effects.

In the electronic configuration eq 1, the 7σ MO mainly describes the lone pair orbital on the C atom, while the 2π MO has the C−C π-bonding and C−O π-antibonding character, as shown in Figure 1. Therefore, a single excitation from the 7σ MO to the 2π MO in eq 4 decreases the CC bond length and increases the CO bond length in the $\tilde{A}\ ^3\Pi$ state, as demonstrated in Figure 4. Correlation effects again elongate the two excited-state bond lengths as much as 0.0132 (1.2739−1.2607) Å for the CC bond and 0.0424 (1.1856−1.1432) Å for the CO bond. It is also observed that the CO bond of the $\tilde{A}\ ^3\Pi$ state is more strongly affected by correlation effects than the CC bond, as was found for the ground state.

According to the schematic potential-energy curves by Choi et al.[15] the lowest energy dissociation channel correlates with the ground state of CO ($\tilde{X}\ ^3\Sigma^-$)

$$\mathrm{CCO}\ (\tilde{X}\ ^3\Sigma^-) \rightarrow \mathrm{C}\ (^3\mathrm{P}) + \mathrm{CO}\ (\tilde{X}\ ^1\Sigma^+) \qquad (13)$$

whereas the $\tilde{A}\ ^3\Pi$ state of CCO correlates with the triplet state of CO ($\tilde{a}\ ^3\Pi$)

$$\mathrm{CCO}\ (\tilde{A}\ ^3\Pi) \rightarrow \mathrm{C}\ (^3\mathrm{P}) + \mathrm{CO}\ (\tilde{a}\ ^3\Pi) \qquad (14)$$

TABLE 4: Theoretical Prediction of the Harmonic Vibrational Bending Frequencies (in cm^{-1}), the Renner Parameter (ϵ), and the ω_2 Bending Frequency (in cm^{-1}) for the $\tilde{A}\ ^3\Pi$ State of CCO

level of theory	$\omega_2^-(\pi^-,A'')$	$\omega_2^+(\pi^+,A')$	ϵ	ω_2
TZ2P EOM-CCSD	666	570	−0.153	620
TZ2P+diff EOM-CCSD	647	553	−0.156	602
TZ3P EOM-CCSD	664	567	−0.156	617
TZ2P(f) EOM-CCSD	683	586	−0.152	636
TZ2P(f)+diff EOM-CCSD	678	586	−0.145	634
TZ3P(2f) EOM-CCSD	674	578	−0.153	627
exptl ref 6 (1971)			−0.172	607.8
exptl ref 11 (1994)			0.176[a]	594.7514(19)

[a] The Renner parameter was evaluated from $\epsilon\omega_2$ (104.4993 cm^{-1}) and ω_2 (594.7514 cm^{-1}) values.

The bond length of the ground state ($\tilde{X}\ ^1\Sigma^+$) and excited triplet state ($\tilde{a}\ ^3\Pi$) of diatomic CO are known to be 1.1283 and 1.2057 Å, respectively.[51] Thus, the CO bond distance for the ground state of CCO is 3.0% *longer* than that of the ground state CO. On the other hand the CO bond length of the first excited triplet state CCO is 1.7% *shorter* than that of the $\tilde{a}\ ^3\Pi$ state of CO. With the most reliable level of theory the sums of the two bond lengths are 2.5326 (1.3699+1.1627) Å for the ground state and 2.4595 (1.2739+1.1856) Å for the first excited triplet state. It is seen that the excited triplet state has a contracted overall structure by 0.0731 (2.5326−2.4595) Å compared to the ground state. This theoretical finding is in excellent agreement with the experimental observation of 0.07 (2.52−2.45) Å contracted structure for the excited triplet state.[6]

B. Dipole Moments. The predicted dipole moment increases with correlation effects for the ground state, while it decreases for the first excited triplet state. At the TZ3P(2f) CISD level of theory, the dipole moments of the ground and first excited triplet states of CCO are 1.42 and 1.47 debye, respectively. It is seen that the $\tilde{A}\ ^3\Pi$ state is slightly more polar than the ground state. Since the magnitude of the dipole moment is considerable, microwave spectroscopic investigations of the ground state are feasible.

C. Harmonic Vibrational Frequencies. The CO stretching frequency (ω_1) is lower for the ground state than for the first excited triplet state, although the CO bond length of the ground state is shorter. The CC stretching frequency (ω_3) is slightly higher for the $\tilde{A}\ ^3\Pi$ state, since the CC bond length is shorter for the $\tilde{A}\ ^3\Pi$ than the $\tilde{X}\ ^3\Sigma^-$ state. The CCO bending frequency ω_2 is degenerate for the ground state, while there are two distinct bending frequencies for the $\tilde{A}\ ^3\Pi$ state. The ground state becomes a $^3A''$ state upon bending. For the $\tilde{A}\ ^3\Pi$ state, however, bending leads to a $^3A''$ and a $^3A'$ state. The $^3A''$ state suffers from a variational collapse to the lower lying $^3A''$ state originating from the linear $\tilde{X}\ ^3\Sigma^-$ state as discussed in section II. This interaction also causes the harmonic bending frequency determined from the $^3A''$ state to be higher than the frequency of the $^3A'$ state. Consequently, the SCF ω_2^- bending frequencies in Table 2 may not be totally reliable. Furthermore, in Table 2 only the $^3A'$ component [ω_2^+] of the bending frequencies are reported for the CISD, CCSD, and CCSD(T) methods. The ω_2^- bending frequencies from the EOM-CCSD technique may be more reliable, at least in a physical and mathematical sense, since the EOM-CCSD wave function is protected from variational collapse.

The harmonic vibrational frequencies of the ground and first excited triplet states of diatomic CO are determined to be 2170 and 1743 cm^{-1}, respectively.[51] The CO stretching (ω_1) frequency of the ground state of CCO is, therefore, 167 cm^{-1} (7.7%) lower than that of the ground state of CO. The corresponding frequency of the first excited triplet state of CCO is 329 cm^{-1} (18.9%) *higher* than that of the $\tilde{a}\ ^3\Pi$ state of CO. Since the theoretically predicted harmonic stretching (ω_1 and ω_3) vibrational frequencies of the $\tilde{X}\ ^3\Sigma^-$ and $\tilde{A}\ ^3\Pi$ states are in close agreement with the experimental fundamental frequencies, the anharmonicity of the stretching modes may be relatively small.

D. Infrared (IR) Intensities. According to the matrix-isolated IR study by Jacox et al.,[4] the IR intensities of the three vibrational modes for the ground state are "strong" for the CO stretch [ν_1 (σ^+)], "medium" for the bend [ν_2 (π)], and "weak" for the CC stretch [ν_3 (σ^+)], respectively. This experimental observation is consistent with our theoretical predictions as shown in Table 1. This feature may be understood through the difference in electronegativity in C and O;[52] C (1.5) and O (3.5). The predicted IR intensitites of the three vibrational modes for the $\tilde{A}\ ^3\Pi$ state show a similar tendency as those for the $\tilde{X}\ ^3\Sigma^-$ state.

E. Renner−Teller Effects. The predicted values for ϵ and ω_2, calculated by neglecting anharmonic terms in the bending potential at the EOM-CCSD level of theory, are shown in Table 4 along with those determined experimentally. Spin−orbit effects were also neglected in the evaluation of the Renner−Teller effects. The sign of ϵ is negative due to the assignment of the V^+ and V^- to the $^3A'$ and $^3A''$ states, respectively, is in agreement with Devillers and Ramsay.[6] There appears to be no clear trend with regard to the basis set employed. For instance, the best agreement with experiment ($\epsilon = 0.176$[53] and $\omega_2 = 594.8$ cm^{-1})[11] is given by the TZ2P+diff EOM-CCSD with $\epsilon = -0.156$ and $\omega_2 = 602$ cm^{-1} and not with the TZ3P(2f) EOM-CCSD, which uses the largest basis employed. Overall the EOM-CCSD method reproduces the Renner−Teller splitting observed from experiment in a reliable manner, thus advocating the method's use in the study of Renner−Teller states.

F. Energetics. With the TZ3P(2f) basis set, the classical $\tilde{X}-\tilde{A}$ splitting for CCO is predicted to be 31.8 (SCF), 33.2 (CISD), 36.4 (EOM-CCSD), 33.2(CCSD), and 33.0 kcal/mol [CCSD(T)] as presented in Table 5. The cc-pVDZ basis set provides similar energetics as the TZ2P+diff basis set, while the cc-pVTZ basis set as the TZ2P(f)+diff basis set. The addition of diffuse functions to the TZ2P and TZ2P(f) basis sets show no significant effect, therefore showing that the first excited triplet state is indeed a true valence state. Since the cc-pVQZ basis set predicts the lowest total energy among the nine basis sets, the energetics from this basis set are considered to be the most reliable. The energy differences determined from the CISD, CCSD, and CCSD(T) methods are remarkably consistent. In our most accurate method, cc-pVQZ CCSD(T), the classical $\tilde{X}-\tilde{A}$ splitting is predicted to be 33.10 kcal/mol (1.435 eV, 11 580 cm^{-1}). Utilizing the TZ3P(2f) CCSD(T) harmonic frequencies from the $\tilde{X}\ ^3\Sigma^-$ state and the TZ3P(2f) CCSD(T) harmonic stretching frequencies with double the TZ3P(2f) EOM-CCSD ω_2 frequency for the $\tilde{A}\ ^3\Pi$ state, the zero-point vibrational energy (ZPVE) correction between the two states becomes 315 cm^{-1}. Consequently, the quantum mechanical

TABLE 5: Excitation Energies (T_e Values, T_0[a] Values in Parentheses) for the $\tilde{A}\ ^3\Pi$ State of CCO Relative to the $\tilde{X}\ ^3\Sigma^-$ State of CCO

level of theory	in kcal/mol
TZ2P SCF	32.20
TZ2P+diff SCF	32.49
TZ3P SCF	32.24
TZ2P(f) SCF	31.65
TZ2P(f)+diff SCF	31.88
TZ3P(2f) SCF	31.75
TZ2P CISD	34.06
TZ2P+diff CISD	34.36
TZ3P CISD	34.12
TZ2P(f) CISD	33.13
TZ2P(f)+diff CISD	33.37
TZ3P(2f) CISD	33.16
cc-pVDZ CISD	34.99
cc-pVTZ CISD	33.74
cc-pVQZ CISD	33.23
TZ2P EOM-CCSD	37.49(38.58)
TZ2P+diff EOM-CCSD	37.80(38.80)
TZ3P EOM-CCSD	37.52(38.59)
TZ2P(f) EOM-CCSD	36.40(37.48)
TZ2P(f)+diff EOM-CCSD	36.65(37.72)
TZ3P(2f) EOM-CCSD	36.44(37.52)
cc-pVDZ EOM-CCSD	38.23(39.31)
cc-pVTZ EOM-CCSD	37.01(38.09)
cc-pVQZ EOM-CCSD	36.42(37.50)
TZ2P CCSD	33.98(34.98)
TZ2P+diff CCSD	34.28(35.23)
TZ3P CCSD	34.04(35.02)
TZ2P(f) CCSD	33.10(34.10)
TZ2P(f)+diff CCSD	33.34(34.33)
TZ3P(2f) CCSD	33.15(34.14)
cc-pVDZ CCSD	34.75(35.74)
cc-pVTZ CCSD	33.75(34.74)
cc-pVQZ CCSD	33.25(34.24)
TZ2P CCSD(T)	33.77(34.84)
TZ2P+diff CCSD(T)	34.07(35.06)
TZ3P CCSD(T)	33.80(34.91)
TZ2P(f) CCSD(T)	32.96(34.02)
TZ2P(f)+diff CCSD(T)	33.21(34.16)
TZ3P(2f) CCSD(T)	33.01(33.91)
cc-pVDZ CCSD(T)	34.57(35.47)
cc-pVTZ CCSD(T)	33.59(34.49)
cc-pVQZ CCSD(T)	33.10(34.00)
exptl ref 6 (1971)	(33.31)[b]
exptl ref 9 (1992)	(33.31)[b]
exptl ref 13 (1996)	(33.85)[b]
exptl ref 14 (1998)	(33.31)[b]

[a] The ZPVE correction for the $\tilde{A}\ ^3\Pi$ state has been included by using the stretching frequencies of the each method and basis set described and then using double the ω_2 value determined at the EOM-CCSD level of theory at the same basis set. The ZPVE correction for the $\tilde{A}\ ^3\Pi$ state for methods utilizing Dunning's correlation consistent basis sets was determined using the TZ3P(2f) stretching frequencies at the corresponding level of theory and double the TZ3P(2f) EOM-CCSD ω_2 value. The ZPVE correction for the $\tilde{X}\ ^3\Sigma^-$ was determined using all frequencies determined at the corresponding level of theory and basis set. [b] The conversion factors used are 349.755 cm^{-1} per kcal/mol and 0.04336411 eV per kcal/mol.

$\tilde{X}-\tilde{A}$ splitting is determined to be 34.00 kcal/mol (1.474 eV, 11 890 cm^{-1}).

Various determinations of the energy splittings have been made over the years. Experimentally, Devillers and Ramsay determined the origin of the $\tilde{A}\ ^3\Pi-\tilde{X}\ ^3\Sigma^-$ transition to be 11 650.80(03) cm^{-1} from the gas-phase absorption spectrum in 1971,[6] Fujitake et al. measured the origin of the $\tilde{A}\ ^3\Pi-\tilde{X}\ ^3\Sigma^-$ band to be 11651.182(14) cm^{-1} by means of near-infrared diode laser spectroscopy in 1992,[9] Zengin et al. found the $\tilde{X}-\tilde{A}$ energy separation to be 1.468(0.015) eV by photoelectron spectroscopy in 1996,[13] and Fulara et al. measured the 0_0^0 band of the $\tilde{A}\ ^3\Pi$ state at 11 650(3) cm^{-1} in the electronic absorption spectrum in 1998.[14] From a theoretical standpoint, Walch in 1980 predicted the $\tilde{X}\ ^3\Sigma^--\tilde{A}\ ^3\Pi$ energy separation to be $T_e = 1.49$ eV using the polarization configuration interaction (POL-CI) technique based on GVB wavefunctions with a plolarized valence double-ζ basis set.[17] Then in 1986, Chabalowski et al. obtained the vertical $\tilde{A} \leftarrow \tilde{X}$ transition energy to be 1.501(1.479) eV using the MRD-CI (full CI estimate) technique with a TZP+diff (64 basis functions) basis set.[18] More recently, in 1996 Zengin et al. determined the $\tilde{X}\ ^3\Sigma^--\tilde{A}\ ^3\Pi$ energy separation to be $T_0 = 1.34$ eV using the CASPT2 method with a (14s9p4d3f/5s4p3d2f) basis set,[13] and in 1999 Choi et al. employed a CASSCF(8,8) wavefunction with the 6-31G* basis set to predict the term value for the $\tilde{A}\ ^3\Pi$ state to be 1.617 eV.[15]

It is clearly seen that our best T_0 value of 34.00 kcal/mol (1.474 eV, 11 890 cm^{-1}) for the $\tilde{X}-\tilde{A}$ splitting is in significantly improved agreement with the experimental T_0 values mentioned above than previous theoretical studies. Furthermore, it should be emphasized that the predicted energies presented in Table 5 are *convergent* to the experimental values in terms of basis set expansion and level of correlation effects.

G. Comparison of EOM-CCSD Results to CCSD and CCSD(T). The EOM-CCSD harmonic vibrational frequencies (see Tables 2 and 4) and geometries (see Figure 4) for the $\tilde{A}\ ^3\Pi$ state of CCO show reasonably good agreement with those from the more reliable CCSD method. The transition energies at the EOM-CCSD level were determined as the energy difference between the CCSD ground state structure and the EOM-CCSD excited state structure. These EOM-CCSD splittings are approximately 3∼4 kcal/mol higher than the CCSD results, which suggests the importance of optimizing the excited state's orbitals in the evaluation of transition energies. Despite this discrepancy, there are some distinct advantages to the EOM-CCSD method. Figure 2 illustrates the ability of this method to resolve the Renner−Teller splitting of the $\tilde{A}\ ^3\Pi$ state in a physically and mathematically correct manner and indeed confirms that $\tilde{A}\ ^3\Pi$ CCO is a Type A Renner−Teller molecule in the classification of Lee et al.[1] Also, as demonstrated earlier in the paper, the method provides reliable Renner−Teller information to compare with experiment, because the method is capable of predicting the ω_2^- π bending frequency without the problem of variational collapse. With the TZ3P(2f) basis set, the ω_2^- π mode is predicted to be 674 cm^{-1} at the EOM-CCSD level of theory. Due to the relatively good agreement between the CCSD and EOM-CCSD results in frequencies and geometries, it is evident that EOM-CCSD may be a viable method for the elucidation of excited states, specifically represented as higher roots of the reference state in the same symmetry. Also its ability to allow for a detailed analysis of Renner−Teller effects make it an ideal method for the study of Renner−Teller molecules.

H. Bond Dissociation Energy for C−CO. The C−CO bond dissociation energies of the ground state CCO presented in eq 13 are shown in Table 6 at the SCF, CCSD, and CCSD(T) levels of theory. It should be noted that these three methods are size consistent. The theoretically predicted bond dissociation energy monotonously increases with the basis set size and the degree of correlation effects. Zengin et al. experimentally determined the C−CO bond dissociation energy in the ground state of CCO to be D_{298K} (C−CO) = 2.29 ± 0.20 eV,[13] whereas Choi et al. determined the C−CO bond dissociation energy to be D_{0K} (C−CO) = 2.24 ± 0.02 eV (51.7 ± 0.5 kcal/mol).[15] With our most

TABLE 6: Bond Dissociation (C−CO) Energies (D_e Values, D_0 Values in Parentheses) for the $\tilde{X}\ ^3\Sigma^-$ State of CCO

level of theory	in kcal/mol	in eV
TZ2P SCF	25.37(22.42)	1.100(0.972)
TZ2P+diff SCF	25.58(22.62)	1.109(0.981)
TZ3P SCF	26.11(23.13)	1.132(1.007)
TZ2P(f) SCF	26.85(23.86)	1.164(1.035)
TZ2P(f)+diff SCF	26.95(23.96)	1.169(1.039)
TZ3P(2f) SCF	27.00(24.02)	1.171(1.042)
TZ2P CCSD	42.35(39.88)	1.836(1.729)
TZ2P+diff CCSD	42.50(40.03)	1.843(1.736)
TZ3P CCSD	43.90(41.37)	1.904(1.794)
TZ2P(f) CCSD	47.65(45.06)	2.066(1.954)
TZ2P(f)+diff CCSD	47.72(45.13)	2.069(1.957)
TZ3P(2f) CCSD	48.57(46.02)	2.106(1.996)
cc-pVDZ CCSD	41.33(38.78)	1.792(1.682)
cc-pVTZ CCSD	47.59(45.04)	2.064(1.953)
cc-pVQZ CCSD	49.37(46.82)	2.141(2.030)
TZ2P CCSD(T)	45.50(43.12)	1.973(1.870)
TZ2P+diff CCSD(T)	45.63(43.22)	1.979(1.874)
TZ3P CCSD(T)	47.07(44.69)	2.041(1.938)
TZ2P(f) CCSD(T)	50.97(48.46)	2.210(2.101)
TZ2P(f)+diff CCSD(T)	51.02(48.41)	2.212(2.099)
TZ3P(2f) CCSD(T)	52.02(49.40)	2.256(2.142)
cc-pVDZ CCSD(T)	44.13(41.51)	1.914(1.800)
cc-pVTZ CCSD(T)	50.96(48.34)	2.210(2.096)
cc-pVQZ CCSD(T)	52.93(50.31)	2.295(2.182)
exptl ref 13 (1996) $D_{0,298K}$	(52.8 ± 4.6)	(2.29 ± 0.20)
exptl ref 15 (1998) $D_{0,0K}$	(51.7 ± 0.5)	(2.24 ± 0.02)

reliable level of theory, cc-pVQZ CCSD(T), the dissociation energy for C−CO is predicted to be 50.31 kcal/mol (2.18 eV), which is good agreement with the experimental values mentioned above.

By comparing the excitation energies in Table 5 and the bond dissociation energies in Table 6, the theoretical dissociation energies are obseved to be more sensitive to the quality of the basis set and the treatments of correlation effects. This feature may be due to the fact that in the dissociation reaction three different species with different spin states are involved, whereas the single electron excitation presented in eq 4 is associated with only one species in two different spatial symmetries.

VI. Concluding Remarks

The ground ($\tilde{X}\ ^3\Sigma^-$) and first excited triplet ($\tilde{A}\ ^3\Pi$) states of the CCO radical have been systematically investigated using high level ab initio electronic structure theory. The optimized geometries, harmonic vibrational frequencies, and associated IR intensities agree quite well with the available experimental values. The EOM-CCSD method has proven useful in the analysis of the Renner−Teller bending mode, allowing the determination of reliable values for the Renner parameter ϵ and the ω_2 bending frequency. At the TZ3P(2f) CCSD(T) level of theory the r_e structures for the two states of the CCO radical are predicted to be r_e (CC) = 1.3699 and r_e (CO) = 1.1627 Å ($\tilde{X}\ ^3\Sigma^-$), and r_e (CC) = 1.2739 and r_e (CO) = 1.1856 Å ($\tilde{A}\ ^3\Pi$), respectively.

In our most reliable method, cc-pVQZ CCSD(T), the classical $\tilde{X}-\tilde{A}$ splitting of CCO is predicted to be 33.1 kcal/mol (1.44 eV, 11600 cm^{-1}) and quantum mechanical splitting to be 34.0 kcal/mol (1.47 eV, 11900 cm^{-1}). These theoretical energy separations are in excellent agreement with the experimental (T_0) value of 11651 cm^{-1}. The present study clearly demonstrates that the CCSD(T) method in conjunction with large basis sets is able to achieve chemical accuracy of 1 kcal/mol in energetics.

Acknowledgment. The authors thank Professor John F. Stanton, Dr. T. Daniel Crawford, and Dr. Wesley D. Allen for their many helpful conversations. The authors thank Dr. Philip R. Bunker for his valuable discussions on the Renner−Teller splitting. This research was supported by the U.S. Department of Energy, Office of Basic Energy Sciences, Division of Chemical Sciences, Fundamental Interaction Branch, Grant DE-FG02-97-ER14748.

References and Notes

(1) Lee, T. J.; Fox, D. J.; Schaefer, H. F.; Pitzer, R. M. *J. Chem. Phys.* **1984**, *81*, 356.
(2) Pitts, W. M.; Donnelly, V. M.; Baronavski, A. P.; McDonald, J. R. *Chem. Phys.* **1981**, *61*, 451.
(3) Ohashi, M.; Suzuki, H.; Ishikawa, S.; Yamamda, C.; Kanamori, H.; Irvine, W. M.; Brown, R. D.; Godfrey, P. D.; Kaifu, N. *Astophys. J.* **1991**, *380*, L39.
(4) Jacox, M. E.; Milligan, D. E.; Moll, N. G.; Thompson, W. E. *J. Chem. Phys.* **1965**, *43*, 3734.
(5) Devillers, M. C. *Compt. Rend. Acad. Sci.* **1966**, *262c*, 1485.
(6) Devillers, M. C.; Ramsay, D. A. *Can. J. Phys.* **1971**, *49*, 2839.
(7) DeKock, R. L.; Weltner, W. *J. Am. Chem. Soc.* **1971**, *93*, 7106.
(8) Smith, G. R.; Weltner, W. *J. Chem. Phys.* **1975**, *62*, 4592.
(9) Fujitake, M.; Kiryu, R.; Ohashi, N. *J. Mol. Spectrosc.* **1992**, *154*, 169.
(10) Ohashi, N.; Kiryu, R.; Okino, S.; Fujitake, M. *J. Mol. Spectrosc.* **1993**, *157*, 50.
(11) Abe, H.; Kikuchi, T.; Takahashi, K.; Fujitake, M.; Ohashi, N. *J. Mol. Spectrosc.* **1994**, *167*, 353.
(12) Abe, H.; Kawamoto, Y.; Fujitake, M.; Ohashi, N.; Momose, T.; Shida, T. *J. Mol. Spectrosc.* **1996**, *180*, 277.
(13) Zengin, V.; Persson, B. J.; Strong, K. M.; Continetti, R. E. *J. Chem. Phys.* **1996**, *105*, 9740.
(14) Fulara, J.; Grutter, M.; Wyss, M.; Maier, J. P. *J. Phys. Chem.* **1998**, *102*, 3459.
(15) Choi, H.; Mordaunt, D. H.; Bise, R. T.; Taylor, T. R.; Neumark, D. M. *J. Chem. Phys.* **1998**, *108*, 4070.
(16) Jacox, M. E. Vibrational and Electronic Energy Levels of Polyatomic Transient Molecules. In *Journal of Chemical Physics Reference Data, Monograph No. 3*; American Institute of Physics: Woodbury, NY, 1994.
(17) Walch, S. P. *J. Chem. Phys.* **1980**, *72*, 5679.
(18) Chabalowski, C.; Buenker, R. J.; Peyerimoff, S. D. *J. Chem. Phys.* **1986**, *84*, 268.
(19) DeKock, R. L.; Grev, R. S.; Schaefer, H. F. *J. Chem. Phys.* **1988**, *89*, 3016.
(20) Maclagan, R. G. A. R.; Sudkeaw, P. *J. Chem. Soc., Faraday Trans.* **1993**, *89*, 3325.
(21) Suter, H. U.; Huang, M.-B.; Engels, B. *J. Chem. Phys.* **1994**, *101*, 7686.
(22) Yamaguchi, Y.; Alberts, I. L.; Goddard, J. D.; Schaefer, H. F. *Chem. Phys.* **1990**, *147*, 309.
(23) Burton, N. A.; Yamaguchi, Y.; Alberts, I. L.; Schaefer, H. F. *J. Chem. Phys.* **1990**, *147*, 309.
(24) Crawford, T. D.; Stanton, J. F.; Allen, W. D.; Schaefer, H. F. *J. Chem. Phys.* **1997**, *107*, 10626.
(25) Renner, R. *Z. Phys.* **1934**, *92*, 172.
(26) Hougen, J. T. *J. Chem. Phys.* **1962**, *36*, 1874.
(27) Herzberg, G. *Molecular Spectra and Molecular Structure III. Electronic Spectra and Electronic Structure of Polyatomic Molecules*; Krieger: Malabara, FL, 1991.
(28) Jungen, C.; Merer, A. J. *Molecular Spectroscopy: Modern Research*; Rao, K. N., Ed.; Academic: New York, 1976; Vol. 2, p 127.
(29) Brown, J. M.; Jørgenson, F. *Adv. Chem. Phys.* **1983**, *52*, 117.
(30) Dixon, R. N. *Phil. Trans. R. Soc. London A* **1960**, *252*, 1007.
(31) Beaton, S. A.; Brown, J. M. *J. Mol. Spectrosc.* **1997**, *183*, 347.
(32) Dunning, T. H. *J. Chem. Phys.* **1971**, *55*, 716.
(33) Huzinaga, S. *J. Chem. Phys.* **1965**, *42*, 1293.
(34) Dunning, T. H. *J. Chem. Phys.* **1989**, *90*, 1007.
(35) Purvis, G. D.; Bartlett, R. J. *J. Chem. Phys.* **1982**, *76*, 1910.
(36) Rittby, M.; Bartlett, R. J. *J. Phys. Chem.* **1988**, *92*, 3033.
(37) Raghavachari, K.; Trucks, G. W.; Pople, J. A.; Head-Gordon, M. *Chem. Phys. Lett.* **1989**, *157*, 479.
(38) Scuseria, G. E. *Chem. Phys. Lett.* **1991**, *176*, 27.
(39) Bunge, A. *J. Chem. Phys.* **1970**, *53*, 20.
(40) Bender, C. F.; Schaefer, H. F. *J. Chem. Phys.* **1971**, *55*, 4789.
(41) Stanton, J. F.; Bartlett, R. J. *J. Chem. Phys.* **1993**, *98*, 7029.
(42) Pulay, P. *Mol. Phys.* **1969**, *17*, 197.
(43) Pulay, P. *Applications of Electronic Structure Theory*; Schaefer, H. F., Ed.; Plenum Press: New York, 1997; Vol. 4, pp 153−185.

(44) Yamaguchi, Y.; Osamura, Y.; Goddard, J. D.; Schaefer, H. F. *A New Dimension to Quantum Chemistry: Analytic Derivative Methods in Ab Initio Molecular Electronic Structure Theory*; Oxford University Press: New York, 1994.

(45) Janssen, C. L.; Seidl, E. T.; Scuseria, G. E.; Hamilton, T. P.; Yamaguchi, Y.; Remington, R. B.; Xie, Y.; Vacek, G.; Sherrill, C. D.; Crawford, T. D.; Fermann, J. T.; Allen, W. D.; Brooks, B. R.; Fitzgerald, G. B.; Fox, D. J.; Gaw, J. F.; Handy, N. C.; Laidig, W. D.; Lee, T. J.; Pitzer, R. M.; Rice, J. E.; Saxe, P.; Scheiner, A. C.; Schaefer, H. F. PSI 2.0.8; PSITECH, Inc., Watkinsville, GA 30677. 1995.

(46) ACES II; Quantum Theory Project; Stanton, J. F.; Gauss, J.; Watts, J. D.; Nooijen, M.; Oliphant, N.; Perera, S. A.; Szalay, P. G.; Lauderdale, W. J.; Gwaltney, S. R.; Beck, S.; Balková, A.; Bernholdt, D. E.; Baeck, K.-K.; Rozyczko, P.; Sekino, H.; Hober, C.; Bartlett, R. J. Integral packages included: VMOL (Almlöf, J.; Taylor, P. R.); VPROPS (Taylor, P.), and ABACUS (Helgaker, T.; Jensen, H. J. Aa.; Jørgensen, P.; Olsen, J.; Taylor, P. R.).

(47) Yamaguchi, Y.; Schaefer, H. F. *J. Chem. Phys.* **1980**, *73*, 2310.

(48) Besler, B. H.; Scuseria, G. E.; Scheiner, A. C.; Schaefer, H. F. *J. Chem. Phys.* **1988**, *89*, 360.

(49) Thomas, J. R.; DeLeeuw, B. J.; Vacek, G.; Schaefer, H. F. *J. Chem. Phys.* **1993**, *98*, 1336.

(50) Thomas, J. R.; DeLeeuw, B. J.; Vacek, G.; Crawford, T. D.; Schaefer, H. F. *J. Chem. Phys.* **1993**, *99*, 403.

(51) Huber, K. P.; Herzberg, G. *Constants of Diatomic Molecules*; van Nostrand Reinhold: New York, 1979.

(52) Pauling, L. *The Nature of the Chemical Bond*, 3rd ed.; Cornell University Press: NY; 1960.

(53) The value for ϵ reported in ref 11 is given as positive due to the authors utilizing equations that did not consider the sign of ϵ. It is clear from this work that the determination by Devillers and Ramsay of ϵ having a negative value is correct.

(54) Yamada, C.; Kanamori, H.; Horiguchi, H.; Tsuchiya, S.; Hirota, E. *J. Chem. Phys.* **1986**, *84*, 2573.

(55) Moassen-Ahmadi, N.; Sandilands, D. W. D.; Boére, R. T. *Chem. Phys. Lett.* **1997**, *265*, 563.